$$\times \left(\frac{d \ln \rho}{d \ln V_s}\right)^{-1}_{sh} \left[\left(\frac{d \ln V_s}{d \ln \rho}\right)_{sh} - \frac{B}{A}\right]^{-1}$$

When calculating temperature and chemical anomalies inside the tectosphere, we use estimates for $(\partial \ln V_s/\partial \ln \rho)_{th}$ to determine effects of temperature variations on V_s. One possibility is to use the velocity-density scaling $(d\ln\rho/d\ln V_s)_{th}$ inferred for the thermal mantle. This approach is internally consistent because it relies entirely on geodynamic constraints. One potential weakness with this approach is the possible presence of partial melting, or thermally induced V_s attenuation in the thermal mantle, making the application of the geodynamically inferred $(d\ln\rho/d\ln V_s)_{th}$ inappropriate in the context of the tectosphere. This leads us to consider an alternative approach in which we use independent mineral physics estimates for $(\partial \ln V_s/\partial \ln \rho)_{th}$. For this purpose, we used an average value of $(\partial \ln V_s/\partial \ln \rho)_{th} \approx 4$ in the upper mantle (*28*). In both approaches, we used the estimate $\delta X_{Gt}/\delta R \sim 4$ [see Fig. 1 in (*7*)] to determine the quantities *A* and *B* defined above. We also assumed a thermal expansion coefficient that varies linearly from $\alpha = 3.3 \times 10^{-5}$ K^{-1} at the top of the mantle to $\alpha = 2.5 \times 10^{-5}$ K^{-1} at the bottom of the upper mantle.

30. We modeled the subcontinental geotherm assuming a steady-state, conductive temperature variation that satisfies a given surface heat flow and also includes distributed radioactive heat sources in the continental crust and in the subcontinental mantle [(*32*), pp. 145–148]. The geotherm was constrained to satisfy an average continental heat flow of 48 mW/m^2, an average crustal thickness of 41 km, an average crustal heat production of 0.77 μW/m^3, and an average mantle heat production of 0.02 μW/m^3 (*9*). These parameters yield a mantle heat flux of 16 mW/m^2 at the base of the continental crust, consistent with previously proposed values (*5*). The average mantle geotherm was modeled with a cooling half-space model [(*32*), pp. 163–167] that was constrained to satisfy a globally averaged mantle heat flow of 65 mW/m^2 (from the weighted average of 16 mW/m^2 in continental regions and 97 mW/m^2 in oceanic regions) and was also constrained to join an average mantle adiabat (with average gradient of 0.36 K/km) that was pinned to a temperature of 1800 K at 400 km depth, corresponding to the phase transition of forsterite to β-Mg_2SiO_4 [A. Chopelas, *J. Geophys. Res.* **96**, 11817 (1991)].
31. S. S. Shapiro, B. H. Hager, T. H. Jordan, *Lithos* **48**, 115 (1999).
32. D. L. Turcotte, G. Schubert, *Geodynamics* (Wiley, New York, 1982).
33. We thank the referees for constructive, useful comments. We also thank the Canadian Natural Sciences and Engineering Research Council and Project LITHOPROBE for their support.

21 September 2000; accepted 10 November 2000

Teleconvection: Remotely Driven Thermal Convection in Rotating Stratified Spherical Layers

Keke Zhang* and Gerald Schubert†

We report the discovery of a convective phenomenon found to occur in a rotating spherical system in which an inner convectively unstable fluid layer is bounded by a corotating outer convectively stable fluid layer. Although convection is thermally driven in the unstable interior, the resulting convective motions concentrate primarily in the stable outer region. This phenomenon, which we term teleconvection, suggests that fluid motions observed at the "surface" of a planet (such as Jupiter's alternating zonal winds) may be driven by an energy source located deep inside the planet.

In many geophysical and astrophysical systems there exist rapid changes in the nature and strength of radial density stratification. Often, a convectively unstable deep interior is surrounded by an outer stably stratified layer (*1*). Convective fluid motions taking place in an unstable fluid may penetrate partially into a neighboring stably stratified region, a phenomenon termed penetrative convection (*2*). The problem of penetrative convection has been extensively studied in various systems [e.g., (*3*); for a review, see (*4*)]. Most studies of penetrative convection have used a nonrotating, plane-layer geometry that cannot capture all the physics of rotating spherical convection. The dynamics of thermal convection in rapidly rotating spherical systems, in which fluid motions are affected by the Coriolis force and spherical geometry, is fundamentally different from that in nonrotating, plane-layer systems (*5–10*). Although penetration into the stable region in a nonrotating convection is weak and spatially restricted (*2, 3*), it can penetrate deeper in a rotating, spherical geometry (*11*).

Planetary and astrophysical convection are usually influenced by spherical geometry, rotation, and the presence of stably stratified layers. Hence, we consider a two-layer convection system: a spherical convectively unstable fluid layer in the region $r_i \le r \le r_m$ characterized by a superadiabatic radial temperature gradient $\partial\Theta_o(r)/\partial r = -|\beta|$, and a spherical convectively stable layer in the region $r_m \le r \le r_o$ characterized by a subadiabatic radial temperature gradient $\partial\Theta_o(r)/\partial r = \delta|\beta|$, where (r, θ, ϕ) are spherical polar coordinates with $r = 0$ at the center of the sphere, Θ_o is the basic temperature field, β is a constant, r_i is the inner radius of the spherical fluid layer, r_m is the interface between the stable and unstable layers, and r_o is the outer radius of the spherical fluid layer. Parameter δ provides a measure of the strength of stable stratification in the outer spherical layer. The whole spherical system rotates uniformly with angular velocity Ω. If $\delta = -1$, the problem is identical to the well-studied convection problem (*12*). When $\delta = 1$, the superadiabatic gradient in the unstable layer has the same amplitude as the subadiabatic gradient in the stable layer. The convection model, apart from spherical geometry and rotation, is essentially the same as penetrative convection models previously studied in plane-layer geometry (*4*). We chose $r_i = r_o/3$ and $r_m = 2r_o/3$ for the purpose of illustration. We also assume that the Boussinesq approximation is valid and the amplitude of convection is so small (the dimensionless velocity $\mathbf{u}$ measured on the viscous time scale is $|\mathbf{u}| \ll 1$) that nonlinear effects can be neglected. It is unlikely that moderate nonlinear effects with $|\mathbf{u}| = O(1)$ (i.e., on the order of 1) would change the key properties of convection in a rapidly rotating spherical system because the effect of rotation is always controlling and dominant (*13*).

In addition to the stratification parameter δ, there are three nondimensional parameters in this convection problem: the Prandtl number *Pr*, the Taylor number *Ta*, and the Rayleigh number *R*, defined as

$$Pr = \frac{\nu}{\kappa} \tag{1}$$

$$Ta = \frac{4\Omega^2(r_o - r_i)^4}{\nu^2} \tag{2}$$

$$R = \frac{g\alpha|\beta|(r_o - r_i)^4}{\nu\kappa} \tag{3}$$

where g is the averaged radial acceleration due to gravity, ν is the kinematic viscosity of the fluid, κ is its thermal diffusivity, and α is its coefficient of thermal expansion; ν, κ, and α are assumed constant and the same in the stable and unstable regions. *Pr* measures the relative efficiency of viscous and thermal diffusion, *Ta* provides a dimensionless measure of the rotation rate, and *R* measures the strength of buoyancy forces in the deep unstable spherical layer $r_i \le r \le r_m$. For planetary atmospheres, *Ta* is usually large ($\gg 1$), whereas *Pr* may be small ($\ll 1$), especially

Department of Earth and Space Sciences and Institute of Geophysics and Planetary Physics, University of California, Los Angeles, CA 90095, USA.

*Present address: School of Mathematical Sciences, University of Exeter, Exeter EX4 4QE, UK.
†To whom correspondence should be addressed.

when radiative processes (*1*) contribute to the effective thermal diffusivity.

When the inner layer is weakly unstable at a small $R \ll O(Ta^{2/3})$, there are no fluid motions and heat transfer is only by conduction; when the inner layer is strongly unstable with a sufficiently large $R = O(Ta^{2/3})$, convection can take place and give rise to a small convective flow ($|\mathbf{u}| \ll 1$) and a small temperature perturbation ($|\Theta| \ll 1$) from the conduction state. It is not only mathematically convenient but also physically intuitive, particularly for the present problem, to express the fluid velocity $\mathbf{u}$ in terms of toroidal $\mathbf{u}_T$ and poloidal $\mathbf{u}_P$ velocity components (*12*)

$$\mathbf{u} = \mathbf{u}_T + \mathbf{u}_P \qquad (4)$$

where $\mathbf{u}_T$ and $\mathbf{u}_P$ are associated with the two scalar functions $T(r, \theta, \phi)$ and $P(r, \theta, \phi)$,

$$\mathbf{u}_T = \left[0, \frac{1}{\sin\theta}\frac{\partial T}{\partial \phi}, -\frac{\partial T}{\partial \theta}\right] \qquad (5)$$

$$\mathbf{u}_P = \left[\frac{L^2 P}{r}, \frac{1}{r}\frac{\partial^2}{\partial\theta\partial r}(rP), \frac{1}{r\sin\theta}\frac{\partial^2}{\partial\theta\partial r}(rP)\right] \qquad (6)$$

and L^2 is the differential operator

$$L^2 = -r^2\nabla^2 + \frac{\partial}{\partial r} r^2 \frac{\partial}{\partial r} \qquad (7)$$

where ∇ is the gradient operator. Equation 4 satisfies the continuity equation and contains the important physics, as described below, for the dynamics of convection in rotating spherical systems. When the system does not rotate ($Ta \equiv 0$), it can be shown that the toroidal flow $\mathbf{u}_T \equiv 0$; when the system rotates rapidly ($Ta \gg 1$), the toroidal and poloidal components become important, usually with $|\mathbf{u}_T| \gg |\mathbf{u}_P|$ (*14*). Furthermore, $\mathbf{u}_T$ does not have a radial component and, hence, it is not directly affected by the presence of a radial stable stratification. Convective states are solutions of the momentum and temperature equations subject to appropriate boundary conditions (*15*). These are solved using the spectral method by expanding T, P, and Θ in terms of the spherical harmonics on a spherical surface and in terms of the Chebychev and sine functions for the radial direction.

When the rate of rotation of the system is sufficiently high ($Ta \gg 1$) and the viscosity of the fluid is sufficiently low ($Pr \ll 1$), we have found that convective fluid motions driven in the interior layer can concentrate mainly in the outer layer. The three-dimensional structure of convective flow and temperature for $Ta = 10^{10}$, $Pr = 0.01$, and $\delta = 1$ shows that the Θ that drives convection concentrates in the inner layer (Fig. 1, A and C). However, convective motions dominated by the toroidal component focus in the stable equatorial region near the outer spherical surface, remote from the inner layer (Fig. 1, B and C). Because of the effect of rotation at $Ta = 10^{10}$, the fluid motions are nearly two-dimensional along the axis of rotation (Fig. 1C). As a result, the stable and unstable regions are associated with two cylinders. The first is tangential to the equator of the inner spherical surface at $r = r_i$ and intersects the outer spherical surface at latitudes Φ of about $\pm 70°$, and the second is tangential to the equator of the interface spherical surface $r = r_m$ and intersects the outer surface at latitudes of about $\Phi = \pm 48°$. The outer spherical surface in the interval $-48° \le \Phi \le 48°$ represents the stable layer in terms of latitudes on the outer spherical surface. The convective motions mainly concentrate in latitudes $-20° < \Phi < 20°$ and are located in the stable region (Fig. 1D). The whole convection pattern drifts in the eastward direction with a phase speed $C = 0.021\ \Omega$ and with a time scale about $100\ \Omega^{-1}$, which is shorter than the viscous diffusion time scale ($10^5\ \Omega^{-1}$) but is longer than the time scale for an inertial wave mode (Ω^{-1}) (*16*).

To provide a quantitative measure of the relative strength of convection in the two layers, we calculate the ratio Q of the kinetic energy of the flow in the stable layer to that in the unstable layer

$$Q = \frac{\int_{r_m}^{r_o}\int_0^{\pi}\int_0^{2\pi} |\mathbf{u}|^2 r^2 \sin\theta\, d\phi\, d\theta\, dr}{\int_{r_i}^{r_m}\int_0^{\pi}\int_0^{2\pi} |\mathbf{u}|^2 r^2 \sin\theta\, d\phi\, d\theta\, dr} \qquad (8)$$

We find that Q is typically about 5 for this type of convection, and that the kinetic energy of the toroidal component in the outer layer is always predominant. Although con-

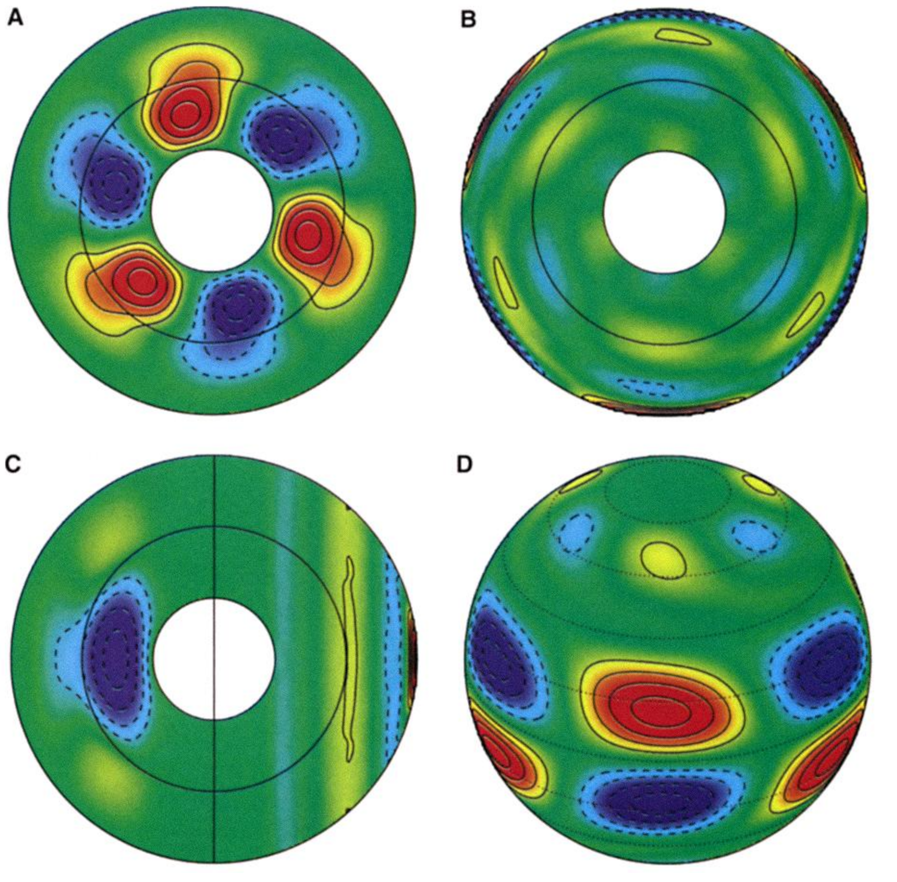

Fig. 1. Temperature and velocity in a rapidly rotating, two-layer spherical system with an inner unstable layer and an outer stable layer, illustrating the phenomenon of teleconvection. (**A** and **B**) Contours of temperature Θ (A) and zonal flow u_ϕ (B) are shown in the equatorial plane. (**C**) Contours of u_ϕ are shown on the right side and contours of Θ are on the left side in a meridian plane. Here the red contours represent positive Θ (or eastward flow), the blue contours are for negative Θ (or westward flow), and the middle solid circle indicates the interface between the stable and unstable regions. (**D**) Streamlines of convective flows on the outer spherical surface at $r = r_o$ viewed at an angle of 30° from the axis of rotation. The latitude circles are given by $\Phi_j = \sin^{-1}(5 - j)/5$, $j = 1, 2, 3, \ldots 7$ with $j = 0$ for the north pole. In the northern hemisphere, the red vortices are cyclones and the blue vortices are anticyclones. The maximum and minimum contour levels are normalized to be 1 and -1, respectively, with the contour intervals decreasing from 0.9 to -0.9 in intervals of 0.2. Dashed lines represent negative contours. The parameters for this solution are $Pr = 0.01$, $Ta = 10^{10}$, and $\delta = 1$.

vection is driven in the inner layer by thermal instability, the fluid motions resulting from the instability concentrate primarily in the outer stable region. Accordingly, we term this phenomenon teleconvection.

Teleconvection is a consequence of the combined effects of rotation, low viscosity, and spherical geometry. In the inner region, convective instability produces a weak poloidal flow in the unstable layer, which penetrates into the outer layer (Fig. 1, B and D). Because of the effects of high rotation and low viscosity (small *Pr*) and the nature of a toroidal flow (which is not affected by the stable stratification), Coriolis forces can produce and amplify a toroidal flow from the weak poloidal flow. The mechanism of teleconvection is in many aspects similar to the alpha-omega dynamo (*17*): A weak poloidal field generated by an alpha effect is amplified by the shear flows through an omega effect to produce a much stronger toroidal magnetic field. In our convection problem, the omega effect resembles the Coriolis forces that generate and amplify the toroidal flow from the weak poloidal flow. The conversion process takes place in both inner and outer layers (*15*), leading to the dominance of the toroidal component in both layers. However, the radial stratification and weaker spherical curvature yield a much larger toroidal flow in the outer layer.

The convective motions concentrate in the outer layer instead of in the inner layer because the infinitesimal steady motions in a rotating inviscid spherical fluid must be two-dimensional with respect to the direction of the rotation axis and must be purely axisymmetric and azimuthal (*12*). This is usually referred to as the rotational or Proudman-Taylor constraint because it must be broken for convection to take place and transport heat. There are generally two different ways to break the rotational constraint: by a large friction force [$O(Ta^{1/3})$ with $Ta \gg 1$] exerted by small-scale [$O(Ta^{-1/6})$] convection cells (*5*), and by unsteadiness of convection in the form of a fast azimuthally traveling wave (*16*). The speed of the convective traveling wave is roughly proportional to the slope of the outer spherical surface (*6*). A reasonably large speed ($C = 0.02\ \Omega$) can be realized only in the stable equatorial region. Consequently, the outer stable equatorial region is the most optimal site for convective flow. The strong effect of rotation and the weak viscous effects allow the toroidal flow to be amplified; the large slope at lower latitudes enables convection to oscillate fast enough to offset the Proudman-Taylor constraint.

As δ increases further from 1, a larger R is needed to initiate convection. Convective motions then take place simultaneously in the stable and unstable layers to form a multilayer structure; this represents a second mode of convection in rotating spherical systems (Fig. 2). For this multilayer convection mode, the ratio of kinetic energies Q is about unity and the amplitude of convection in the stable equatorial region is about the same as that in the unstable region. Although convection is still driven only in the inner layer, convective motions concentrate in two separate locations: the Busse-type rolls in the unstable layer and the zonal flows in the outer stable equatorial region (Fig. 2, C and D). In this case, the whole pattern drifts at a lower phase speed with $C = 0.014\ \Omega$. The two convection modes we report are a consequence of the radial stratification, without which they cannot take place.

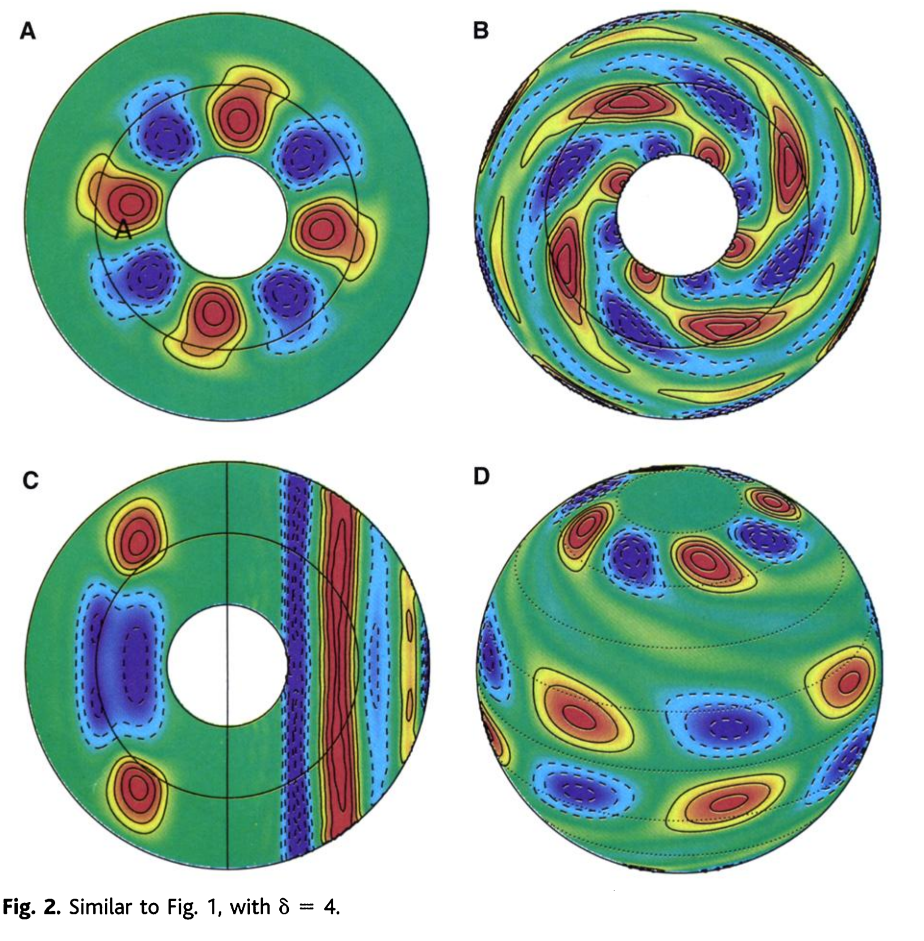

Fig. 2. Similar to Fig. 1, with $\delta = 4$.

Nearly a quarter of a century ago, F. H. Busse (*18*) proposed a weakly nonlinear convection model for the atmosphere of Jupiter on the basis of an assumption that there exist multilayer convection rolls similar to those shown in Fig. 2, C and D. He suggested that the nonlinear interactions between different convection rolls can produce alternating mean zonal flows like those observed in the atmosphere of Jupiter (*18, 19*). Since then, the problem of thermal convection in rotating spherical systems without a stable layer has been extensively studied [e.g., (*7, 8, 10, 20*)], but the multilayer roll structure of Busse's model has not been found for either linear or weakly nonlinear convection. We have found a mechanism that breaks the single long spiraling convection roll (*14*) and forms a multilayer roll structure. Our model suggests that a multilayer roll structure of convection, similar to the one suggested by Busse, can take place in a rotating, weakly nonlinear, multilayer spherical convective system.

Of course, teleconvection cannot take place when the stratification parameter δ becomes too large. We can estimate the critical value of δ at which normal convection would occur by noting that it is the dynamic dominance of the Coriolis force that causes the phenomenon of teleconvection. When the negative buoyancy force in the stable region is comparable to the Coriolis force there, we expect that teleconvection would disappear. By equating the negative buoyancy force $R\Theta$ to the Coriolis force $Ta^{1/2}\mathbf{k} \times \mathbf{u}$ and using the heat equation, we obtain

$$\delta \sim Ta^{1/2}m^2/R \qquad (9)$$

where m is the azimuthal wavenumber of convection. Taking $m \sim Ta^{1/6}$ and $R \sim Ta^{2/3}$ [see (*5*)], we obtain

$$\delta = O(Ta^{1/6}) \qquad (10)$$

at which convection would be mainly confined in the unstable inner region. The estimate in Eq. 10 is confirmed by our calculations, which show that convection adopts a normal convective pattern with weak penetration for $Ta = 10^{10}$ when $\delta \geq O(10)$. In the case of the jovian atmosphere, if we take $Ta = 10^{12}$ for Jupiter (*9*), we obtain $\delta = 100$.

Teleconvection may have important implications for the dynamics of planetary and stellar atmospheres and interiors. According to the structural models of Jupiter by Guillot *et al.* (*1*), regions in the outer part of Jupiter's atmosphere may be stable against convection. Although Earth's liquid core is convectively unstable to convection [e.g., (*5, 6, 17, 21*)] and generates a magnetic field, the outermost part of Earth's core may be stably stratified [e.g., (*22*)]. Our findings suggest that the flows observed on Jupiter (*23, 24*) or the core flows near Earth's core-mantle boundary inferred from geomagnetic observations may be driven by thermal forcing in inner unstable regions rather than by thermal forcing at the sites of the motions themselves. Generally speaking, whenever a convective system is characterized by rapid rotation, low viscosity, and spherical geometry, teleconvection can occur. Convective fluid motions observed on an outer spherical surface may be driven by a deep energy source.

References and Notes

1. T. Guillot, D. Gautier, G. Chabrier, B. Mooser, *Icarus* **112**, 337 (1994).
2. G. Veronis, *Astrophys. J.* **137**, 641 (1963).
3. R. D. Baker, G. Schubert, P. W. Jones, *J. Atmos. Sci.* **55**, 3 (1998).
4. B. Straughan, *Mathematical Aspects of Penetrative Convection* (Longman Scientific, New York, 1993).
5. P. H. Roberts, *Philos. Trans. R. Soc. London Ser. A* **263**, 93 (1968).
6. F. H. Busse, *J. Fluid Mech.* **44**, 441 (1970).
7. K. Zhang, F. Busse, *Geophys. Astrophys. Fluid Dyn.* **39**, 119 (1987).
8. Z. P. Sun, G. Schubert, G. A. Glatzmaier, *Geophys. Astrophys. Fluid Dyn.* **69**, 95 (1993).
9. J. B. Manneville, P. L. Olson, *Icarus* **122**, 242 (1996).
10. C. A. Jones, A. M. Soward, A. I. Mussa, *J. Fluid Mech.* **405**, 157 (2000).
11. K. Zhang, G. Schubert, *Science* **273**, 941 (1996).
12. S. Chandrasekhar, *Hydrodynamic and Hydromagnetic Stability* (Clarendon, Oxford, 1961).
13. A. Tilgner, F. H. Busse, *J. Fluid Mech.* **332**, 359 (1997).
14. K. Zhang, *J. Fluid Mech.* **236**, 535 (1992).
15. *P*, *T*, and Θ are governed by three nondimensional equations,
$$[(\nabla^2 - \partial/\partial t)L^2 + Ta^{1/2}\partial/\partial\phi]\nabla^2 P + Ta^{1/2}DT - RL^2\Theta = -\mathbf{r}\cdot\nabla\times\nabla\times(\mathbf{u}\cdot\nabla\mathbf{u})$$
$$[(\nabla^2 - \partial/\partial t)L^2 + Ta^{1/2}\partial/\partial\phi]T - Ta^{1/2}DP = \mathbf{r}\cdot\nabla\times(\mathbf{u}\cdot\nabla\mathbf{u})$$
$$(\nabla^2 - Pr\partial/\partial t)\Theta + L^2(P/r)\partial\Theta_0/\partial r = Pr\mathbf{u}\cdot\nabla\Theta$$
where the differential operator *D* is defined as
$$D = \mathbf{k}\cdot\nabla - \tfrac{1}{2}(L^2\mathbf{k}\cdot\nabla + \mathbf{k}\cdot\nabla L^2)$$
with **k** a unit vector along the polar axis in the direction of rotation. Nonlinear terms on the right side of the above equations are neglected in our calculations. We impose impenetrable, perfectly thermally conducting, and stress-free boundary conditions
$$P = \Theta = \partial^2 P/\partial r^2 = \partial/\partial r(T/r) = 0$$
at the spherical surfaces $r = r_i$ and $r = r_o$. After applying the standard procedure of the spectral method, convection solutions described by *T*, *P*, Θ, the critical Rayleigh number, and the drift rate are obtained by a nonlinear iterative method (*16*).
16. K. Zhang, *J. Fluid Mech.* **268**, 211 (1994).
17. H. K. Moffatt, *Magnetic Field Generation in Electrically Conducting Fluids* (Cambridge Univ. Press, Cambridge, 1978).
18. F. H. Busse, *Icarus* **20**, 255 (1976).
19. ———, *Geophys. Astrophys. Fluid Dyn.* **23**, 152 (1983).
20. M. Ardes, F. H. Busse, J. Wicht, *Phys. Earth Planet. Inter.* **99**, 55 (1997).
21. P. Olson, J. Aurnou, *Nature* **402**, 170 (1999).
22. D. Gubbins, C. J. Thomson, K. A. Whaler, *Geophys. J. R. Astron. Soc.* **68**, 241 (1982).
23. P. J. Gierasch *et al.*, *Nature* **403**, 628 (2000).
24. A. Seiff, *Nature* **403**, 603 (2000).

25. Supported by a Particle Physics and Astronomy Research Council and National Science Foundation of China grant (K.Z.) and by the NASA Planetary Atmospheres Program (G.S.).

25 August 2000; accepted 30 October 2000

Rapid Changes in the Hydrologic Cycle of the Tropical Atlantic During the Last Glacial

Larry C. Peterson,[1]* Gerald H. Haug,[2] Konrad A. Hughen,[3] Ursula Röhl[4]

Sedimentary time series of color reflectance and major element chemistry from the anoxic Cariaco Basin off the coast of northern Venezuela record large and abrupt shifts in the hydrologic cycle of the tropical Atlantic during the past 90,000 years. Marine productivity maxima and increased precipitation and riverine discharge from northern South America are closely linked to interstadial (warm) climate events of marine isotope stage 3, as recorded in Greenland ice cores. Increased precipitation at this latitude during interstadials suggests the potential for greater moisture export from the Atlantic to Pacific, which could have affected the salinity balance of the Atlantic and increased thermohaline heat transport to high northern latitudes. This supports the notion that tropical feedbacks played an important role in modulating global climate during the last glacial period.

Large millennial-scale air temperature oscillations first observed in the oxygen isotopic composition ($\delta^{18}O$) of Greenland ice reflect massive reorganizations of the atmosphere-ocean system during the last glacial period (*1*). A growing number of records show that their importance was global in scope (*2*). In the search for mechanisms, attention has increasingly focused on the tropics because of their potential to alter the oceanic balance of heat and fresh water, in addition to their role as a source of water vapor to the atmosphere (*3*). Although precise documentation of changing tropical hydrologies is critical to furthering our understanding of rapid climate variations, only a few locations around the world provide appropriate recorders. Here, we present a multiproxy sediment record of subcentennial resolution that is interpreted to reflect variations in ocean productivity and precipitation patterns over northern South America during the past 90,000 years (90 ky).

The Cariaco Basin is located in a region that is highly sensitive to climate change. Today, upwelling of cold nutrient-rich waters occurs along the northern Venezuelan coast in response to trade wind changes that accompany the seasonal migration of the Intertropical Convergence Zone (ITCZ). The movement of the ITCZ also imposes a wet and dry season on the region, with rainfall variations affecting rivers that deliver terrigenous sediment and nutrients to the western North Atlantic and southern Caribbean. Cariaco Basin sediments record a history of this upwelling and riverine runoff (*4–6*) and offer the opportunity to reconstruct past changes in the tropical ocean and atmosphere and in the hydrologic balance over northern South America.

We report results from Ocean Drilling Program (ODP) Site 1002 (10°42.73′N, 65°10.18′W), drilled at a water depth of 893 m in the basin. The 170-m sediment sequence is continuous and spans the time interval from 0 to ~580,000 years ago (580 ka) (*7*); only data from the uppermost 36 m of Hole 1002C, spanning the period from 0 to 90 ka, are presented here. Terrigenous components compose a large fraction of the sediments (35 to 90 weight %) (*7*) because of the proximity to the South American margin, with variable contributions from nannofossils, foraminifers, diatoms, and pteropods. High sedimentation rates (averaging 40 cm/ky) result in an important tropical counterpart to high-latitude ice cores for the study of rapid climate change.

[1]Rosenstiel School of Marine and Atmospheric Science, University of Miami, Miami, FL 33149, USA. [2]Department of Earth Sciences, Swiss Federal Institute of Technology (ETH), CH-8092 Zürich, Switzerland. [3]Woods Hole Oceanographic Institution, Woods Hole, MA 02543, USA. [4]Fachbereich Geowissenschaften, Universität Bremen, D-28334 Bremen, Germany.

*To whom correspondence should be addressed. E-mail: lpeterson@rsmas.miami.edu